



## Real-Time Device-Level Data Fusion Method for Enhanced Monitoring in Distributed Energy Grids

Yue Chen<sup>1</sup>, Chenghui Liu<sup>1</sup>, Fangfang Zhou<sup>1</sup>, Kun Zhang<sup>1</sup> and Yingyu Lin<sup>1</sup>

<sup>1</sup> Guangdong Power Grid Co, 510000 China

**SUMMARY:** *Due to the large number of access nodes, complex equipment levels and strong asynchrony of multi-source data in distributed energy grid, traditional monitoring methods are difficult to meet the requirements of high-precision perception and low-delay response at the same time. This paper proposes a device-level real-time data fusion method for augmented monitoring. This paper focused on IEEE 1588 time synchronization, sliding window resampling, quality-aware unified representation, Conv1D local feature extraction, GRU state modeling, Softmax adaptive weighted fusion, edge-side lightweight gated temporal network inference, ring buffer queue and cloud-edge parameter synchronization mechanism. A closed-loop computation link from data alignment, state estimation to local execution output is constructed. The experimental results show that in the simulation scene composed of 8 photovoltaic inverters, 5 smart meters and 12 groups of sensors, the monitoring accuracy of the proposed method reaches 96.5%, the F1-score reaches 95.7%, the average response delay is reduced to 54 ms, and the F1-score of 84.6% is still maintained under the condition of 20% noise and 20% packet loss. It shows that the proposed method can provide reliable support for high-precision real-time perception, edge collaborative processing and intelligent decision-making of distributed energy grid.*

**KEYWORDS:** *Distributed energy grid; Device level; Real-time data fusion; Enhance monitoring*

## 1 Introduction

Under the background of accelerated construction of new energy system and continuous promotion of intelligent distribution side, distributed energy grid is gradually evolving from a single energy supply unit to an open cooperative system integrating power generation, energy storage, load response and edge control [1]. Compared with the traditional centralized power grid, such systems have more access nodes, more complex equipment levels, more significant two-way coupling between power flow and information flow, and more dynamic, discrete and uncertain operation states [2, 3]. Inverters, smart meters, frequency recording devices, and various environmental and electrical sensors continuously generate multi-source heterogeneous data, which provides a rich information basis for operation monitoring, anomaly identification and local regulation. However, it also makes the monitoring system face practical problems such as inconsistent sampling frequency, timestamp drift, obvious noise disturbance and limited computing resources on the edge side [4].

Existing research has focused on smart meter data analysis, multi-source information fusion, abnormal state detection and grid operation and maintenance data integration, and has

\*CZ153678@163.com

<https://doi.org/10.65102/is2026801>

made certain progress in improving the accuracy of state perception and assisting dispatch decision-making [5, 6]. Existing methods have shown that data fusion is an important technical path to enhance monitoring capabilities [7]. However, there are still several weak points in realizing real-time monitoring data fusion from the device level. First, the upload cycle and time reference of different devices are quite different, and it is difficult to stably align high-frequency and low-frequency data on a unified logical timeline. Secondly, communication interruption, electromagnetic interference and buffer overflow can cause missing, mutation and abnormal zero values, which directly affect the credibility of the fusion results. Third, some methods pay more attention to offline analysis or center-end processing, and lack of consideration for low-latency execution, lightweight reasoning and online adaptation of edge nodes, which is difficult to meet the needs of rapid monitoring in complex scenarios [8-10].

Aiming at the above problems, this paper focuses on the device-level real-time data fusion task in distributed energy grid, and studies the unified processing and collaborative execution method for enhanced monitoring. Based on the data acquisition and clock synchronization of multi-source devices, this paper introduces a unified time reference mechanism based on IEEE 1588 precision time protocol, and constructs a standardized input stream by combining sliding window and frame alignment strategy. On this basis, aiming at the problems of equipment state fluctuation, noise pollution and timing mismatch, a state estimation model for real-time perception is established, which integrates running state representation, abnormal symptom capture and uncertainty assessment into the same computing framework. Furthermore, an adaptive weighted fusion mechanism is constructed by combining the device confidence, state consistency and historical stability, so that the fusion results can be dynamically adjusted according to the data quality and timing characteristics. Finally, for the needs of edge deployment, lightweight network, cache queue and local inference execution are adopted to reduce the scale of model parameters and calculation delay, and improve the practicability of the algorithm on the device side of the field.

The research goal of this paper is to form a device-level enhanced monitoring scheme that takes into account monitoring accuracy, response speed and robustness. Compared with traditional single-source monitoring or static weighted fusion methods, the proposed method emphasizes the collaborative relationship between time synchronization, state modeling, dynamic weight update and edge real-time execution, and tries to maintain the continuity, accuracy and interpretability of monitoring output under complex disturbance conditions. This study helps to promote the distributed energy grid from "data access" to "data understanding" and "real-time response", and also provides more reliable data basis and method support for subsequent local control, fault warning and cloud-edge collaborative decision-making.

## 2 Related work

Focusing on the enhanced monitoring and device-level data processing of distributed energy grid, existing research mainly focuses on abnormal attack recognition, edge computing support, phasor data cleaning, distributed energy cooperative control, and intelligent monitoring system construction. Irfan et al. systematically sorted out the detection and location of false data injection attacks in smart grid, indicating that the monitoring system should not only pay attention to the accuracy of physical quantity collection, but also have the ability to identify abnormal data sources [11]. Starting from the smart grid perception scenario, Cardenas et al. discussed the modeling and simulation problem for edge computing alliance, reflecting that the computing power sink to the location close to the data source has

become a critical path to improve real-time performance [12]. Khaledian et al. used Isolation Forest, KMeans and LoOP to realize anomaly detection and classification of synchronous phasor data, indicating that multi-model collaboration can improve the identification ability of complex anomaly patterns [13]. Gholami et al. combined filtering, clustering and Koopman modal analysis to suppress noise and detect bad data in distribution phasor measurement, indicating that the quality of data preprocessing directly affects the subsequent state perception effect [14].

In terms of edge-side intelligent processing and distributed energy collaborative sensing, Mehmood et al. summarized edge computing in iot smart grid, and pointed out that low latency, local decision making and communication load reduction are important advantages of edge architecture [15]. Muller et al. studied the event correlation process of distributed energy resources from the perspective of cyber-physical event reasoning, and emphasized the role of state evolution understanding in distributed energy monitoring [16]. Vosughi et al. further reviewed the cyber-physical vulnerability and resilience issues under distributed energy access, indicating that the monitoring system needs to take into account data credibility, system disturbance immunity and operation recovery capabilities at the same time [17]. Nikam et al. reviewed the control strategy of microgrid containing distributed energy, energy storage and electric vehicles, reflecting that the scenario of coexistence of multiple types of devices puts forward higher requirements for unified monitoring and collaborative regulation [18]. Adham et al. and Hargroves et al. reviewed from the perspective of overall research on distributed energy resources and decentralized energy transformation, respectively, and revealed that equipment diversification, decentralized access and autonomous operation have become important features of current energy systems [19, 20].

Looking further, Lakshmi Satya Nagasri et al. summarized the advanced control technology of microgrid, indicating that real-time perception, dynamic regulation and local autonomy are deeply integrated [21]. Islam et al. discussed the application of machine learning in power system stability and control, indicating that data-driven modeling has become an important method for operation state analysis [22]. Guato Burgos et al. reviewed the artificial intelligence methods in smart grid anomaly detection, showing that anomaly recognition is evolving from rule analysis to intelligent recognition [23]. Ojo et al. summarized the control strategy and real-time monitoring system of microgrid, further highlighting the integration trend of monitoring, control and online feedback [24]. Alvarez-Alvarado et al. reviewed the cyber-physical power system from the perspectives of technology driving, standard system and future development, indicating that heterogeneous data collaborative processing has become an important foundation to support complex power grid operation [25]. Alrowaili et al. reviewed the situation awareness and critical asset identification of smart grid cyber-physical system and emphasized that enhanced monitoring needs to be extended from single-point measurement to global perception [26]. Menazzi et al. verified the significance of real-time data integration on system resilience improvement from the perspective of power outage management and data-driven real-time aggregation of distributed energy resources [27].

In general, existing research provides basic support for distributed energy monitoring, such as anomaly recognition, edge computing, event reasoning, and intelligent control. However, most of the results are more focused on attack detection, system review, or aggregation level analysis, and there is still a lack of integrated methods for deal-level real-time data alignment, unified representation, adaptive fusion, and edge collaborative execution. Based on this, this paper further studies the device-level real-time data fusion method for enhanced monitoring scenarios to improve the perception accuracy, response

speed and operation robustness of distributed energy grid under complex disturbance conditions.

### 3 Design of device level real-time data fusion method for enhanced monitoring in distributed energy grid

#### 3.1 Timing alignment and unified representation of multi-source heterogeneous data at the device level

The device level data in distributed energy grid has the characteristics of dispersed sources, obvious differences in sampling frequency, inconsistent timestamp accuracy and heterogeneous data semantics. Inverters usually upload active power, voltage and current information at the frequency of seconds or even higher, smart meters usually update measurement data at a frequency lower than the inverter, and environmental and electrical sensors often return state variables such as frequency, temperature and harmonics in the second or subsecond level. If such raw data are directly used for subsequent fusion calculations, it is easy to cause problems such as inconsistent observation at the same time, amplification of timing dislocation and imbalance of feature dimension, which ultimately affect the accuracy of enhanced monitoring results. Based on this, under the framework of device-side and edge-side collaboration, this paper constructs a temporal alignment and unified representation method for multi-source heterogeneous data, which integrates time calibration, resampling mapping, quality coding and tensorization organization into the same processing link, so as to provide a consistent data base for subsequent state estimation and adaptive fusion.

In order to reduce the time deviation caused by the local clock drift of the device and the jitter of network transmission, this paper uses the edge gateway as the unified reference clock and combines the IEEE 1588 precision time synchronization mechanism to correct the upload timestamp of each device. Let the original timestamp of the type  $i$  device at the  $k$ -th report be  $t_i^{(k)}$  and the corresponding clock offset be  $\delta_i^{(k)}$ , then the modified logical time can be expressed as follows:

$$\tilde{t}_i^{(k)} = t_i^{(k)} + \delta_i^{(k)} \quad (1)$$

where  $\delta_i^{(k)}$  is estimated online from the offset between the reference clock and the device clock. Considering that the clock offset will vary with the communication delay and load fluctuation during the operation of the device, this paper further uses a recursive smoothing strategy to update the offset:

$$\delta_i^{(k+1)} = \rho \delta_i^{(k)} + (1-\rho)(t_r^{(k)} - t_i^{(k)}) \quad (2)$$

where,  $t_r^{(k)}$  is the reference clock time and  $\rho \in [0,1]$  is the smoothing factor. This processing can continuously suppress the cumulative error of time drift without significantly increasing the computational burden on the edge side, so that heterogeneous device data can be mapped to a unified logical timeline.

After completing the time calibration, aiming at the coexistence of high frequency sampling and low frequency sampling, this paper designs an adaptive window resampling mechanism to normalize the data of different devices to a fixed fusion period  $\Delta\tau$ . For low-frequency data, local linear interpolation was used to supplement the observations in the

current fusion window. For high-frequency data, the dominant dynamic characteristics are retained by window aggregation. Let the original observation sequence of device  $i$  be  $x_i(t)$ , and the unified mapping value at logical time  $\tau$  be defined as follows:

$$\bar{x}_i(\tau) = \begin{cases} x_i(t_a) + \frac{\tau - t_a}{t_b - t_a} [x_i(t_b) - x_i(t_a)], f_i < f_0 \\ \frac{1}{|W_\tau|} \sum_{t \in W_\tau} x_i(t), f_i \geq f_0 \end{cases} \quad (3)$$

Here,  $f_i$  is the original sampling frequency of device  $i$ ,  $f_0$  is the unified fusion frequency threshold, and  $W_\tau$  is the sliding time window centered at  $\tau$ . The expression preserves the continuous trend of low-frequency sequences and the local statistical characteristics of high-frequency sequences at the same time, avoiding information loss caused by simple up-sampling or down-sampling.

Considering that the device data may have missing, abnormal mutation and noise pollution during transmission, this paper introduces a quality-aware coding mechanism to attach validity markers and confidence scores to the feature values at each time step. Let  $m_i(\tau) \in \{0,1\}$  denote whether the data is valid at the current time, and  $q_i(\tau) \in [0,1]$  denote the data quality score obtained by the combination of missing rate, noise rate and repair ratio. Then the unified representation vector of device  $i$  is written as follows:

$$z_i(\tau) = [\bar{x}_i(\tau), m_i(\tau), q_i(\tau)] \quad (4)$$

On this basis, the representation results of all devices at the same time step are further concatenated into a unified input matrix, and then combined with a sliding window of length  $L$  to construct a 3D input tensor:

$$X_\tau = [Z_{\tau-L+1}, Z_{\tau-L+2}, \dots, Z_\tau] \in \mathbb{R}^{L \times N \times D} \quad (5)$$

where  $N$  is the number of devices and  $D$  is the single device representation dimension. Different from the traditional input organization method that only preserves the numerical values of physical quantities, the tensor encapsulates the time-aligned observations, data availability and quality weight information at the same time, so that the subsequent model can perceive numerical changes, identify observation confidence, and maintain better fault tolerance for abnormal sampling in the same computational framework.

Figure 1 shows the process of multi-source heterogeneous device data timing alignment and unified representation. This process is not only oriented to the device heterogeneity in distributed energy scenarios, but also takes into account the real-time processing requirements of the edge side, and can be used as the standard input interface for subsequent state estimation models and adaptive fusion algorithms.

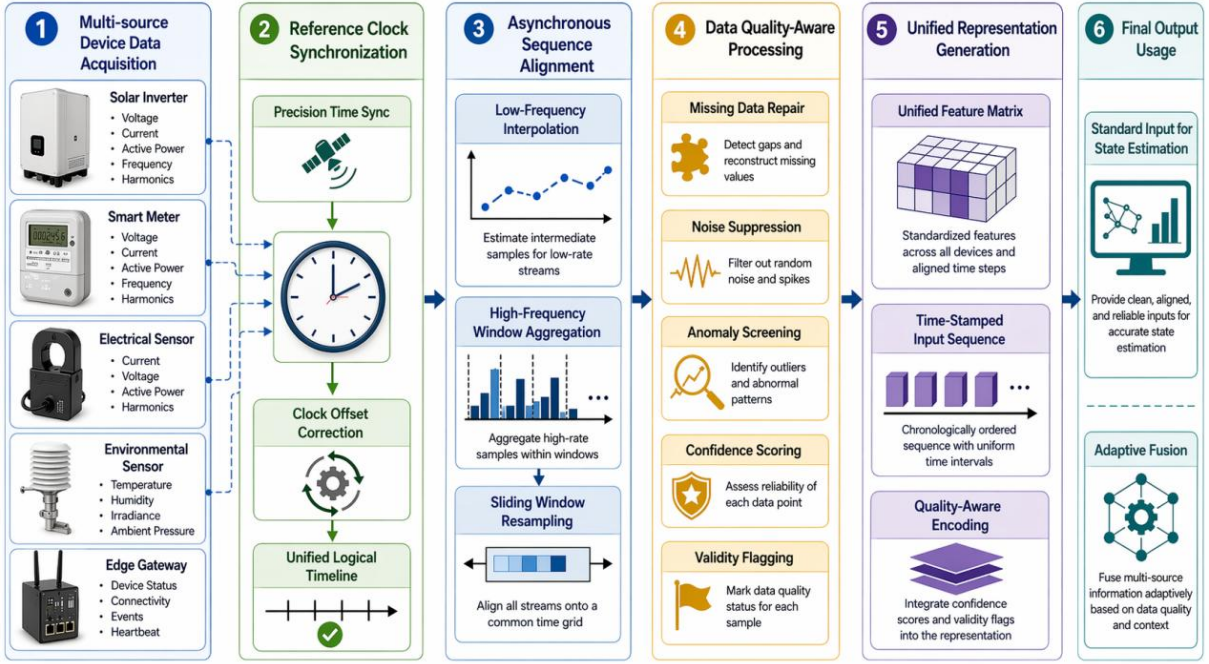


Figure 1: Flow chart of timing alignment and unified representation of multi-source heterogeneous device data

In summary, this section completes the front-end organization of multi-source data at the device level from three levels: time calibration, frequency unification, and structured coding, which not only compresses the time error caused by asynchronous sampling, but also improves the semantic and structural consistency of input features, laying a foundation for the design of data fusion algorithms for real-time perception and state representation in the next section.

### 3.2 Device-level data fusion algorithm design for real-time perception and state representation

After the time series alignment and unified representation of multi-source heterogeneous device data are completed, the key of device level data fusion is to extract state evolution features in continuous time Windows, identify the observation confidence of each device, and map them into a unified state output that can be used to enhance monitoring. Considering the characteristics of distributed energy grid, such as fast power fluctuation, multiple disturbance sources, and unstable device upload rhythm, this paper introduces a calculation link of "local timing encoder-state representation generation -adaptive weight allocation -fusion result output" in the algorithm design, and combines lightweight convolution with gated recurrent unit. A device level fusion model that considers both edge reasoning efficiency and dynamic perception ability is constructed.

Aiming at the problems of obvious short-time mutations and strong local waveform differences in the unified input tensor, this paper first uses one-dimensional causal convolution to extract local dynamic features, and then uses GRU to complete the cross-time step state memory update. Let the input of the  $\tau$  th fusion window be  $X_\tau$ , the local encoding result be  $e_\tau$ , and the hidden state be  $h_\tau$ . Then the state representation generation process is written as follows:

$$e_\tau = \sigma(\text{Conv1D}(X_\tau) + b_e) \quad (6)$$

$$h_t = \text{GRU}(e_t, h_{t-1}), z_T = W_z h_T + b_z \quad (7)$$

Here,  $z_t$  is the device level state representation vector of the current window, which not only retains the local disturbance information, but also encodes the short-term operation trend. Compared with the fusion method that only relies on the original measurements, this structure of "convolution to extract local and cycle to capture evolution" is more suitable for describing the dynamic state of the inverter under the joint action of power fluctuation, frequency offset and environmental disturbance.

In order to avoid excessive influence of one device on the fusion result due to abnormal sampling, communication lag or local noise, this paper introduces an adaptive weight calculation mechanism based on the state representation. The device weight is no longer set as a fixed constant, but is jointly determined by five factors: data quality, state consistency, time freshness, historical stability and anomaly penalty. In order to facilitate subsequent implementation, this paper arranges the calculated attributes and action relationships of each factor as shown in Table 1.

*Table 1: Adaptive fusion weight calculation factor and function description table*

Calculation Factor	Typical Value Range	Typical Coefficient	Basis for Calculation	Effect on Fusion Results
Data Quality Score	0.60–1.00	0.34	Jointly evaluated from missing rate, noise rate, and repair ratio	Higher data quality leads to a larger base weight for device observations in the fusion process
State Consistency	0.50–1.00	0.27	Degree of matching between current observations and state representation outputs	Stronger consistency indicates that the device can better reflect the true system state
Temporal Freshness	0.40–1.00	0.19	Calculated from upload latency and deviation from the current fusion window	The closer the data are to the current time, the higher the priority for real-time perception
Historical Stability	0.45–1.00	0.12	Estimated from fluctuation variance and continuous validity rate within a sliding window	Higher stability implies more reliable long-term contribution
Anomaly Penalty Term	0.00–0.35	0.08	Derived from outlier scores, abrupt-change intensity, and rule-check results	The higher the anomaly level, the more significantly the corresponding weight is suppressed

The coefficients given in Table 1 are used as the initial configuration for online update, which can be further fine-tuned according to the operating load and error feedback of edge nodes in different scenarios. Based on this setting, the integrated reliability of the  $i$ th device at time  $\tau$  is defined as follows:

$$r_i(\tau)=0.34q_i(\tau)+0.27c_i(\tau)+0.19f_i(\tau)+0.12s_i(\tau)-0.08p_i(\tau) \quad (8)$$

After obtaining the comprehensive reliability, this paper uses Softmax normalization with effective masks to generate dynamic fusion weights. If  $m_i(\tau)$  indicates whether the device is currently uploading, its weight can be written as follows:

$$\alpha_i(\tau)=\frac{m_i(\tau)\exp(r_i(\tau)/T)}{\sum_{j=1}^N m_j(\tau)\exp(r_j(\tau)/T)} \quad (9)$$

where,  $T$  is the temperature coefficient, which is used to adjust the sharpness of the weight distribution. When the system enters the working condition with strong disturbance or more local packet missing, the equipment with higher reliability will automatically obtain a larger contribution proportion, and the influence of distorted observation will be suppressed at a low level.

In the fusion output stage, this paper jointly maps the device observation vector and the state representation vector to form the final enhanced monitoring result. Let  $x_i(\tau)$  be the current observation feature of the  $i$ th device and  $\hat{y}_\tau$  be the fusion output, then we have:

$$\hat{y}_\tau = \sum_{i=1}^N \alpha_i(\tau)\phi(x_i(\tau), z_\tau) \quad (10)$$

Here,  $\phi(\cdot)$  represents the lightweight mapping function, which can be realized by the combination of linear layer and gating unit. In order to balance real-time accuracy and output smoothness, supervised loss and temporal consistency constraints are further constructed in the training phase:

$$L=\|\hat{y}_\tau-y_\tau^*\|_2^2+\lambda\|\hat{y}_\tau-\hat{y}_{\tau-1}\|_2^2+\mu\sum_{i=1}^N \alpha_i(\tau)p_i(\tau) \quad (11)$$

Here,  $y_\tau^*$  is the reference monitoring label,  $\lambda$  is used to constrain the continuous window output jitter, and  $\mu$  is used to penalize the residual effect of highly abnormal devices in the fusion. Such an objective function makes the model not only pursue the monitoring value approaching the true state, but also actively control the output continuity and the risk of anomaly propagation, which is more in line with the stability requirements of enhanced monitoring in engineering scenarios.

In general, the dep-level data fusion algorithm constructed in this section is not a static average of multi-source observations, but an online reconstruction of the contribution of devices through timing coding, state representation and dynamic weighting. The proposed method can maintain high real-time perception ability under the condition of limited edge resources, and provide direct algorithmic support for the implementation mechanism of enhanced monitoring based on real-time data fusion and edge collaborative execution in the next section.

### 3.3 Implementation mechanism of enhanced monitoring based on real-time data fusion and edge collaborative execution

After the device-level temporal alignment, unified representation and adaptive fusion calculation are completed, whether the enhanced monitoring can really be implemented depends on whether the fusion results can achieve low-latency execution, event-level

response and cloud-edge collaborative update on the edge side. The distribution of inverters, smart meters, environmental sensors and edge gateways in distributed energy grid is discrete. If the serial path of "full uploading-central processing-result return" is still adopted, it is easy to generate sensing hysteresis under the conditions of communication congestion, local disturbance enhancement and concurrent reporting by multiple nodes. Based on this, this paper constructs an enhanced monitoring implementation mechanism of "edge cache-real-time reasoning-event discrimination-local executing-cloud synchronization", which couples the fusion output with the edge scheduling logic, so that the monitoring results can directly serve the local alarm, equipment adjustment and status reporting.

The data access layer of the edge node uses a ring buffer queue to maintain continuous time Windows, writes the uniform input sequence from different devices in a rolling manner according to the length of the window, and generates a real-time task description vector for each window. Considering that anomaly degree, time freshness, data uncertainty and queue backlog status all affect edge processing priority, this paper defines the priority score of monitoring tasks as follows:

$$S_{\tau} = \lambda_1 A_{\tau} + \lambda_2 F_{\tau} + \lambda_3 U_{\tau} + \lambda_4 B_{\tau} \quad (12)$$

where  $A_{\tau}$  represents the anomaly intensity of the current window,  $F_{\tau}$  represents the time freshness,  $U_{\tau}$  represents the uncertainty of the fusion result,  $B_{\tau}$  represents the task backlog degree in the edge cache, and  $\lambda_1 \sim \lambda_4$  is the priority adjustment coefficient. The higher this score is, the more the current window needs to be prioritized for reasoning and fast output.

In the execution layer, the edge gateway adaptively schedules the inference frequency according to the priority score. If  $\Delta t_0$  represents the base execution period, the actual execution interval of the current window can be written as follows:

$$\Delta t_{\tau}^{\text{exec}} = \frac{\Delta t_0}{1 + \kappa S_{\tau}} \quad (13)$$

Here,  $\kappa$  is the regulation gain. The execution interval of Windows with high abnormal intensity, fast data update or large uncertainty will be compressed, so as to improve the response speed under transient conditions. The stationary condition maintains a longer execution period to reduce the edge resource occupation. This mechanism is relatively simple in calculation and suitable for deployment on the gateway side with limited computing power. Figure 2 shows the edge collaborative execution and enhanced monitoring output mechanism.

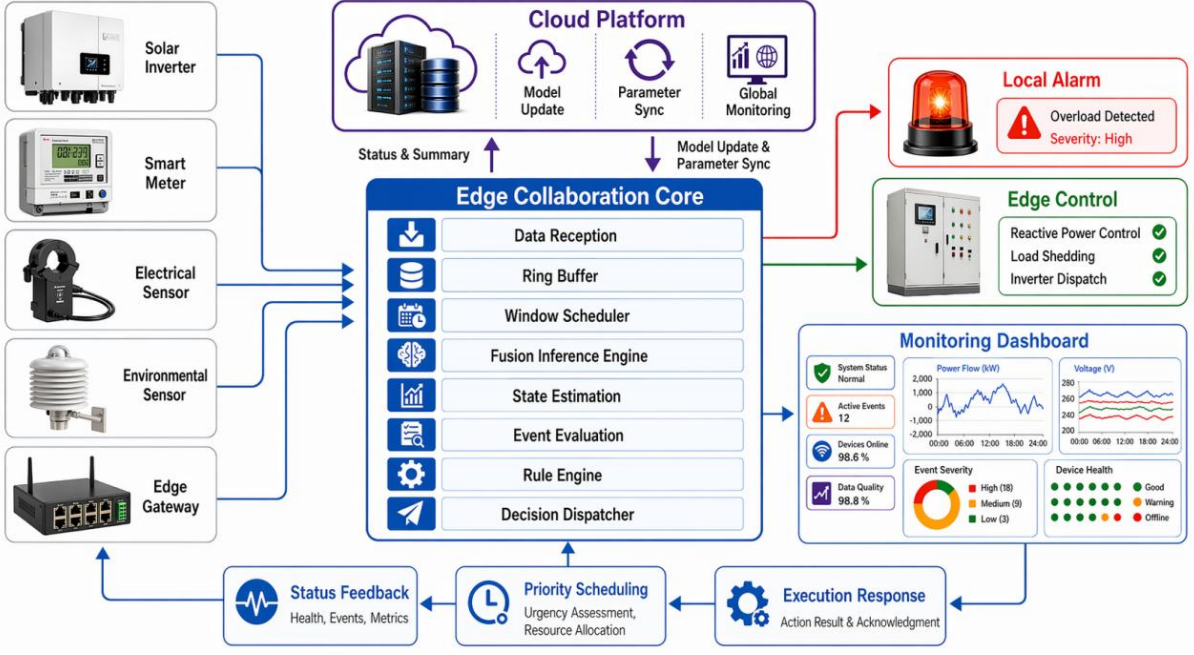


Figure 2: Edge collaborative execution and enhanced monitoring output mechanism diagram

The mechanism shown in Figure 2 highlights the synergistic relationship between immediate processing at the edge side and multipath output, enabling enhanced monitoring to move further into the real-time response level.

In order to map the fusion results into executable monitoring outputs, this paper introduces the monitoring output intensity function, which integrates the state estimates, event confidence and rule constraints into the output calculation process. Let  $\hat{y}_\tau$  be the fusion output of the current window,  $C_\tau$  be the event confidence score, and  $R_\tau$  be the rule verification result, then the enhanced monitoring output is defined as follows:

$$o_\tau = \psi(\hat{y}_\tau) + \beta C_\tau + \gamma R_\tau \quad (14)$$

where  $\psi(\cdot)$  represents the nonlinear mapping to the fusion result,  $\beta$  and  $\gamma$  are the weight coefficients of event confidence and rule constraint. The output not only retains the sensitivity of the data-driven model to complex state changes, but also absorbs the rapid discrimination ability of the edge rule engine for problems such as over-limit, mutation and equipment mismatch, so it is more suitable for on-site enhanced monitoring scenarios.

In the cloud-edge collaboration layer, we do not let the edge nodes run independently for a long time, but maintain the consistency of the cloud model and the edge model through a lightweight parameter transmission mechanism. Let the edge side parameters be  $\Theta_\tau^e$  and the cloud reference parameters be  $\Theta_\tau^c$ , then the edge parameter update rule is written as follows:

$$\Theta_{\tau+1}^e = \Theta_\tau^e - \eta \nabla L_\tau^e + \mu (\Theta_\tau^c - \Theta_\tau^e) \quad (15)$$

Here,  $\eta$  is the edge learning step,  $L_\tau^e$  is the local loss of the current window, and  $\mu$  is the consistency adjustment coefficient of cloud edges. The former term ensures that the edge model can be fine-tuned online according to field data, and the latter term suppresses excessive drift of the edge model due to local sample bias. In this way, it not only retains the ability of rapid adaptation of the edge side, but also maintains the stability of the overall system model.

In the specific implementation, the edge node divided the enhanced monitoring output into three levels of response: mild anomalies directly triggered the local prompt and status marking, moderate anomalies linkage device control interface to perform clipping or resampling, and high-grade anomalies were uploaded to the cloud scheduling platform while retaining the local emergency strategy. Due to the integrated design of local caching, lightweight reasoning, priority scheduling and result distribution, the closed-loop feedback of monitoring results can be completed in a shorter path, and the transmission time from data to action can be significantly shortened. The implementation mechanism proposed in this section further transforms the real-time data fusion results into the executable, synchronized and scalable enhanced monitoring output, which provides the implementation basis for the application verification and performance analysis in Chapter 4.

## **4 Application verification of device-level real-time data fusion method for enhanced monitoring**

### **4.1 Distributed energy grid simulation scenarios and construction of multi-type equipment data sets**

In order to verify the applicability of the proposed device level real-time data fusion method in enhanced monitoring, this paper builds a simulation experiment platform for distributed energy grid, and completes multi-source data access, standardized processing and unified input organization at the edge gateway side. A total of 8 PV inverter nodes, 5 smart meters and 12 groups of environmental and electrical sensors are configured in the experimental scene, forming a multi-type equipment data set covering the generation side, the metering side and the sensing side. The original variables collected by each node include voltage, current, active power, frequency and temperature, etc. The sampling frequency of the inverter is 1 kHz, the smart meter is 10 Hz, and the sensor is 5 Hz, which can better reflect the characteristics of heterogeneous, asynchronous and multi-scale of equipment data in distributed energy scenarios. All data are uploaded to the edge gateway uniformly, and the gateway performs timestamp calibration, tensor construction and fusion input generation. Four working conditions, namely steady state operation, power mutation, data missing caused by abnormal communication and random noise injection, are set up to investigate the adaptability of the method under complex disturbances. The preprocessing results show that when the random missing rate is 10%-25%, the accuracy of abnormal data repair remains above 90%, and the noise standard deviation decreases by about 37% after filtering, which indicates that the constructed data set not only has the characteristics of equipment level monitoring, but also can provide a reliable data basis for subsequent accuracy, delay and robustness verification. The dataset and device sampling configuration are shown in Table 2.

Table 2: Data set and device sampling configuration table

Device Type	Main Monitoring Variables	Sampling Frequency	Number of Nodes	Data Usage
Photovoltaic Inverter	Voltage, current, active power, frequency	1 kHz	8	Reflects power output and electrical state fluctuations on the generation side
Smart Meter	Voltage, current, active power, harmonic-related information	10 Hz	5	Characterizes metering-side operating features and load variations
Environmental and Electrical Sensor Group	Temperature, frequency, current, and environmental sensing information	5 Hz	12	Provides supplementary observations of environmental disturbances and local operating states
Edge Gateway	Multi-source data aggregation status, cache, and upload information	Real-time access	1	Responsible for time synchronization, data standardization, and fusion input construction
Typical Operating Conditions	Steady-state operation, power mutation, communication anomalies, random noise injection	—	4 types	Used to verify the adaptability and robustness of the method under complex scenarios

## 4.2 Multi-source equipment data preprocessing process and experimental parameter configuration

In order to ensure that the sampling results of different devices can enter the same fusion computing framework, a preprocessing process of "time synchronization, exception repair, noise suppression, standardized mapping, window organization" is constructed at the edge gateway side. After all the original data arrive at the gateway, the unified clock calibration is completed based on the IEEE 1588 Precision Time protocol, and the time error tolerance is set to be less than 20 ms. The data frames beyond the threshold are not involved in the current fusion cycle to avoid the amplification of asynchronous bias in the subsequent state estimation. Then, linear interpolation was used to complement the low-frequency upload data, and sliding window aggregation was used to aggregate the high-frequency fluctuation data, so that the data with different sampling frequencies were uniformly mapped into a fixed fusion period. Aiming at the missing, mutation and abnormal zero values caused by communication interruption, electromagnetic interference and buffer overflow, this paper adopts the combination repair strategy of "trend interpolation + neighborhood replacement + history replay", and retains repair labels for the reconstructed samples for subsequent dynamic weight adjustment.

In the noise suppression stage, bandpass filtering and median filtering were combined for continuous analog quantities such as voltage and current, where the median filtering window length was set to 5. For the slow-varying disturbance such as temperature drift, the exponential moving average is introduced for smooth update. When the proportion of noise or missing exceeds 30% in a single sampling period, the segment of data is placed into the mask area and does not directly participate in the current round of fusion to ensure stable input quality. To quantify the availability of pre-processed samples, the data quality score of the  $\tau$

fusion window is defined as follows:

$$Q_{\tau}=1-(\alpha r_{\tau}^m+\beta r_{\tau}^n+\gamma r_{\tau}^a) \quad (16)$$

Here,  $r_{\tau}^m$  represents the missing ratio,  $r_{\tau}^n$  represents the noise ratio,  $r_{\tau}^a$  represents the time mismatch ratio,  $\alpha$ ,  $\beta$ ,  $\gamma$  are the weight coefficients, and satisfies  $\alpha+\beta+\gamma=1$ . When  $Q_{\tau}$  is lower than the set threshold, this window only retains the state reference effect and does not enter the main fusion channel. The design makes the preprocessing results not only complete data cleaning, but also form a quality prior that can directly participate in the subsequent adaptive fusion.

In terms of experimental parameter configuration, the update period of the unified input stream was set from 500 ms to 1 s, and the length of the sliding window was configured as a short window according to the real-time requirements. The edge-side state estimation sub-model adopts a two-layer lightweight gating structure, and the parameter scale is controlled within 10K, and the single inference delay is controlled within 20 ms. The fusion logic module was supported by the local circular cache queue to avoid repeated memory allocation. In the ARM Cortex-A55 processor environment, the execution time of a single round of fusion is controlled within 80 ms. The results are transmitted by UDP broadcast to reduce the handshake overhead and improve the output efficiency in high-frequency update scenarios. After processing, the multi-source device data can be converted into a standard input sequence driven by a unified timestamp, which provides a stable data basis for subsequent accuracy analysis and edge execution verification.

### 4.3 Comparative analysis of enhanced monitoring accuracy under different fusion methods

In order to verify the recognition advantages of the proposed method in equipment level enhanced monitoring, this paper compares the single-source monitoring, static weighted fusion and the adaptive fusion method in this paper under the same data set and the same working conditions, and focuses on the accuracy of key state recognition and the changes of related accuracy indicators. The comparison of monitoring accuracy indicators of different fusion methods is shown in Figure 3.

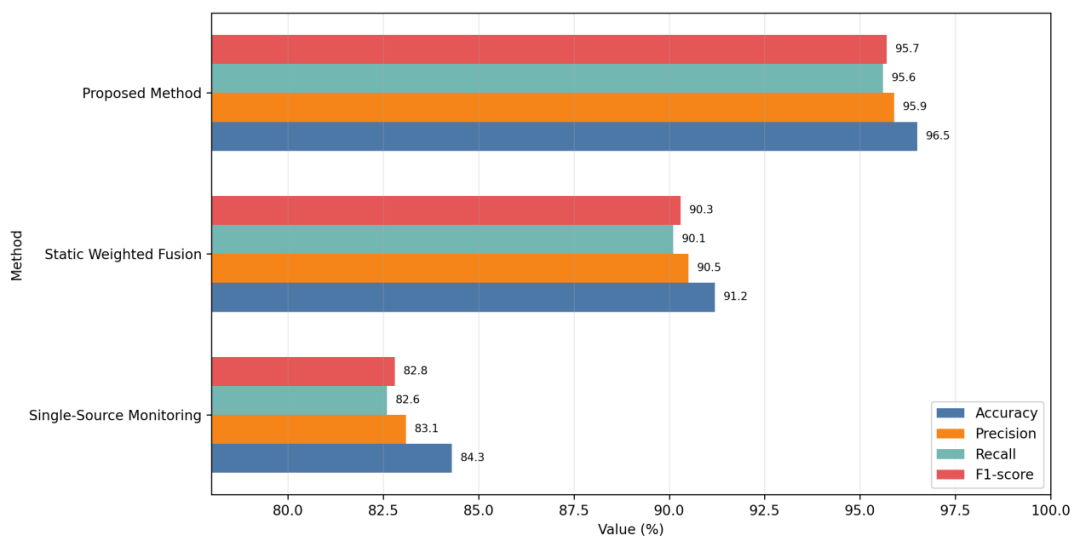


Figure 3: Grouped bar charts comparing monitoring accuracy indicators of different fusion methods

As shown in Figure 3, with the enhancement of the fusion level and the ability of dynamic weight adjustment, the recognition ability of the monitoring model to the states such as voltage anomaly, power fluctuation and frequency drift shows a continuous improvement trend. Among them, the average accuracy of the single source monitoring method is 84.3%, the static weighted fusion method is increased to 91.2%, and the proposed method further reaches 96.5%, which is 12.2 percentage points and 5.3 percentage points higher than that of the single source monitoring and the static weighted fusion, respectively. At the same time, the Precision, Recall and F1-score reach 95.9%, 95.6% and 95.7% respectively, which are better than the other two methods as a whole, indicating that the proposed method has higher monitoring accuracy and more stable anomaly identification ability in complex operating scenarios.

#### 4.4 Real-time Response Performance and execution efficiency verification for edge deployment

In order to further verify the real-time response ability and execution stability of the proposed method under the condition of edge deployment, this paper compares the single-source monitoring and static weighted fusion with the proposed method deployed in the same edge gateway environment, focusing on the distribution characteristics of response delay and the change of execution efficiency under the condition of multi-index coupling. Figure 4 shows the distribution of edge response time delay for different methods.

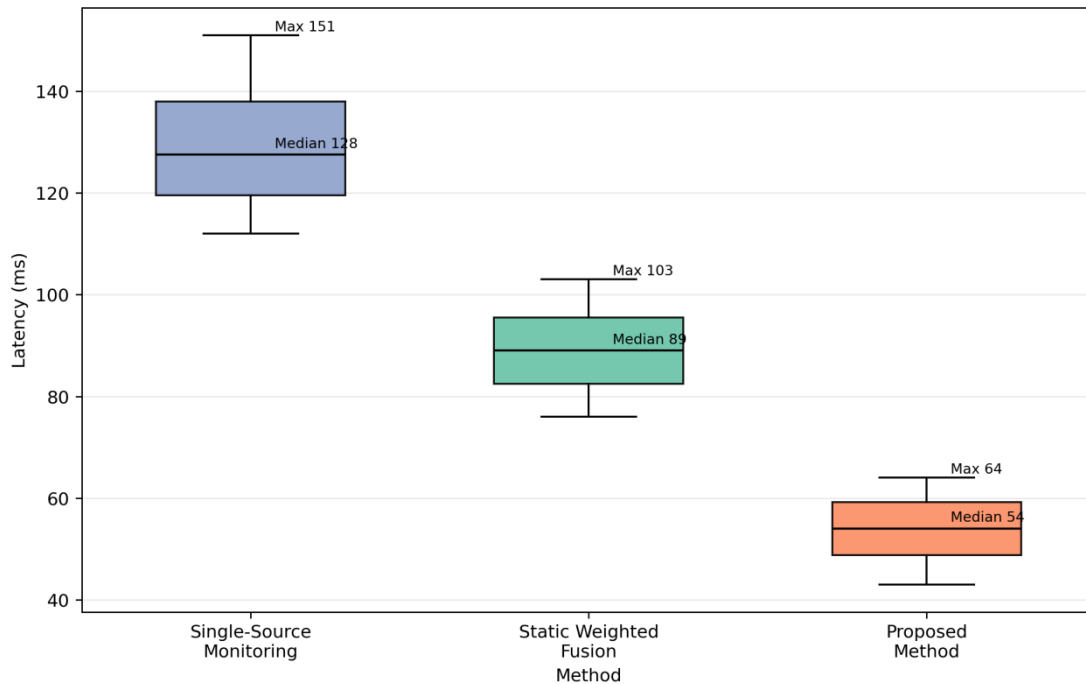


Figure 4: Boxplot of edge response time delay distribution for different methods

As shown in Figure 4, the delay distribution of the single-source monitoring method is generally high, with a median response delay of about 128 ms and a maximum delay of 151 ms, indicating that its overall response efficiency is relatively weak due to the lack of unified fusion processing and priority scheduling mechanism under the condition of multi-source concurrent input. The median delay of the static weighted fusion method is reduced to 89 ms, and the overall fluctuation range is reduced, but there is still a certain degree of dispersion. The median response delay of the proposed method is further compressed to 54 ms, and the

maximum delay is controlled within 64 ms, and the box interval is significantly narrower. The results show that the proposed method can not only significantly reduce the response delay, but also has better execution stability and real-time processing ability under edge deployment conditions. The multi-index comparison of edge execution efficiency is shown in Figure 5.

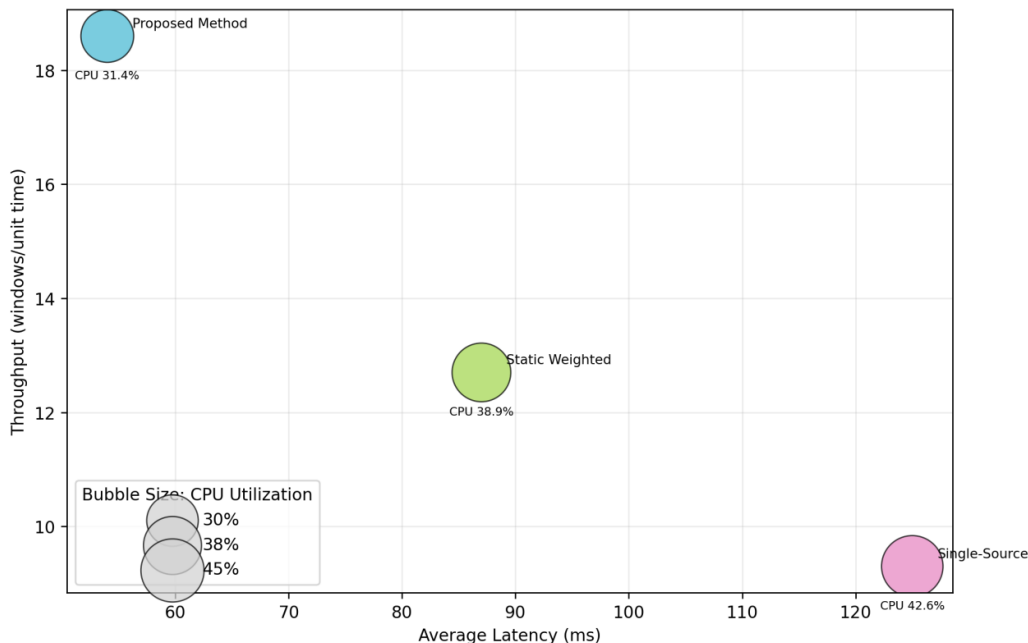


Figure 5: Edge execution efficiency multi-metric bubble plot

As shown in Figure 5, the single-source monitoring method is located in the area of high latency and low throughput, with an average response delay of 125 ms, 9.3 Windows can be processed per unit time, and the CPU occupancy rate reaches 42.6%. The average delay of the static weighted fusion method was reduced to 87 ms, the processing power was increased to 12.7 Windows, and the CPU occupancy rate was 38.9%. The average response delay of the proposed method is 54 ms, the number of Windows per unit time reaches 18.6, and the CPU occupancy rate is controlled at 31.4%. It can be seen that the proposed method not only has obvious advantages in the delay index, but also achieves a better balance between throughput and resource consumption, which indicates that it is more suitable for deployment in edge gateway scenarios with limited computing power but high real-time requirements.

#### 4.5 Robustness and anti-interference ability evaluation of fusion method under complex disturbance conditions

In order to further investigate the stability and anti-interference ability of the proposed method in complex disturbance scenarios, this paper adds different intensities of noise disturbances and communication packet loss disturbances on the basis of the original test set, and uses F1-score to characterize the change of fusion performance. Figure 6 shows the fusion performance variation under complex disturbance conditions.

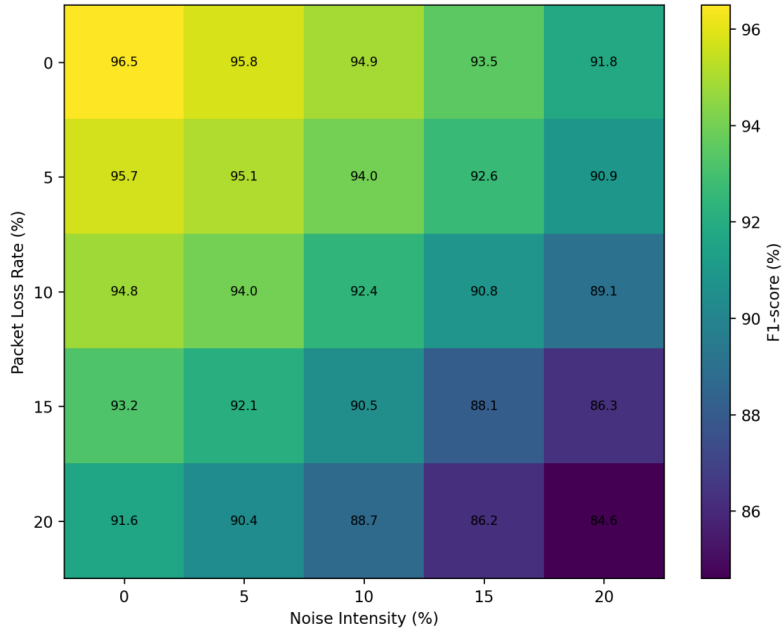


Figure 6: Heat map of fusion performance change under complex disturbance conditions

As shown in Figure 6, as the noise intensity and packet loss rate increase synchronously, the overall fusion performance shows a downward trend, but the decline process is relatively gentle. When the noise intensity and packet loss rate are both 0, the F1-score of the model is 95.7%. When both of them increased to 10%, the F1-score remained at 92.4%. When the perturbation is further increased to 15%, the F1-score is 88.1%. Under the compound disturbance of 20% noise and 20% packet loss, F1-score still reaches 84.6%. This shows that the proposed method can still maintain good monitoring accuracy under the condition of medium and high intensity interference, indicating that the front-end unified representation, dynamic weight adjustment and real-time update mechanism at the edge side have a strong inhibition effect on abnormal data propagation. The comparison of abnormal state response curves before and after fusion is shown in Figure 7.

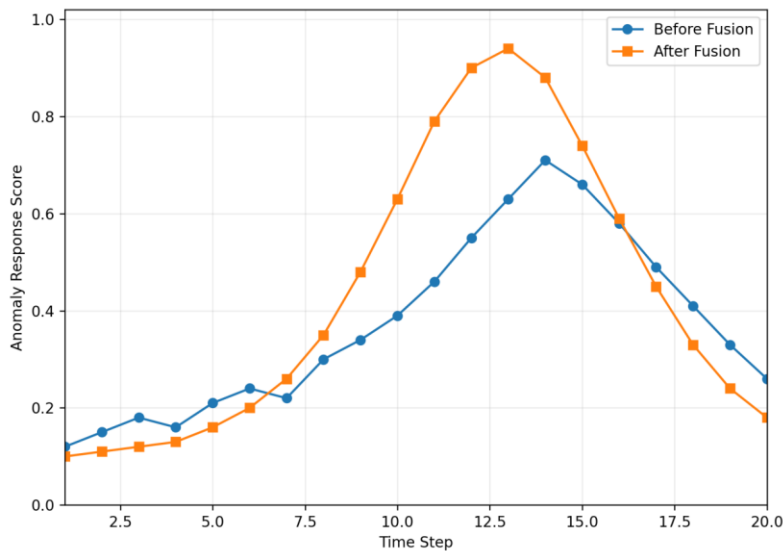


Figure 7: Comparison of abnormal state response curves before and after fusion

As shown in Figure 7, the response curve of abnormal state before fusion is greatly affected by noise disturbance, and the fluctuation is obvious in the early rising stage. The peak appears in the 14th time step, and the response score is 0.71. After fusion, the overall curve is smoother, and the abnormal response starts to accelerate from the 8th time step, and reaches the peak of 0.94 at the 13th time step, which is 0.23 higher than that before fusion, and the increase is about 32.4%. At the same time, the retreat phase after the end of the anomaly is more stable, and the terminal residual response decreases from 0.26 to 0.18. The results show that after real-time data fusion, the model is more sensitive to the response of abnormal states, positioning is clearer, and anti-noise ability is stronger. It can maintain better stability of anomaly recognition and reliability of edge monitoring in complex disturbance scenes.

## 5 Discussion

From the overall results, the device-level real-time data fusion method constructed in this paper shows good synergy advantages in the three dimensions of monitoring accuracy, edge response speed and robustness under complex disturbances. This result shows that the enhanced monitoring in the distributed energy grid cannot only rely on the observation of a single device, nor can it stay in the static weighted data superposition, but should form a continuous closed loop around "time unification, state representation, dynamic fusion, edge execution". The timing alignment and unified representation method proposed in chapter 3 essentially solves the problems of sampling frequency inconsistency, time drift and data semantic fragmentation between multi-source heterogeneous devices, so that the subsequent state estimation model has a more stable input basis. On this basis, the adaptive fusion mechanism takes data quality, state consistency, time freshness and historical stability into the weight allocation process, so that the fusion results can be adjusted online with the change of running state. This is also the key reason why the proposed method achieves 96.5% accuracy, 95.9% Precision, 95.6% Recall, and 95.7% F1-score in monitoring.

Furthermore, the proposed method still maintains good real-time performance under the condition of edge deployment, which is particularly important for distributed energy scenarios. The traditional centralized monitoring method is prone to response lag under the conditions of concurrent uploading of multiple nodes, local disturbance bursts and communication link fluctuations, and there is a long transmission link between data and decision. In this paper, through edge caching, window scheduling, lightweight reasoning and local result distribution, the fusion computing and execution logic are connected in a closed-loop at the gateway side, so that the monitoring output can directly serve for alarm triggering, edge control and cloud synchronization. In the experiment, the average response time of the proposed method is reduced to 54 ms, the median response time is maintained around 54 ms, and the maximum delay is controlled within 64 ms. At the same time, the number of processing Windows per unit time is increased to 18.6, which shows that the proposed method still has high execution efficiency in the computing power constrained environment. This means that the proposed method is not only suitable for experimental environments, but also has the engineering potential to migrate to actual edge gateways, station side controllers, and area monitoring nodes.

In terms of anti-jamming ability, the proposed method shows strong stability. The heatmap results show that, although the fusion performance decreases when the noise intensity and packet loss rate increase at the same time, the decline slope is relatively gentle. Even with the composite perturbation of 20% noise and 20% packet loss, the F1-score remains at 84.6%. The response curve of abnormal states also shows that the peak value of the curve after fusion is higher, the rise is more concentrated, and the fall is smoother, indicating that the method

has stronger focusing ability for key abnormal states. This phenomenon shows that the dynamic weight adjustment mechanism does not only improve the accuracy in the average sense, but also improves the ability of the model to screen effective information when abnormal samples, missing samples and noise samples exist together. For the distributed energy grid, this capability has strong practical significance, because the data quality in the actual scenario often fluctuates continuously, and the monitoring system needs to have the ability to tolerate incomplete information and contaminated information.

Of course, there are some limitations in this paper. At present, the equipment scale, scene complexity and network topology of the experimental platform are still relatively limited, and the verification of large-scale distributed node cooperation, cross-regional edge cluster joint execution and long-cycle online evolution conditions are not sufficient. The lightweight state estimation and fusion structure adopted in this paper is more suitable for the current experimental conditions. However, when extreme disturbances, the further increase of device types or the concurrency of monitoring tasks are significantly improved, the model parameter scheduling, buffer management and cloud-edge synchronization frequency may still face new pressures. Future research can further introduce more fine-grained edge task scheduling mechanisms, parameter compression and incremental update strategies, and combine more complex cyber physical scenarios to conduct in-depth evaluation of system scalability, adaptive ability and long-term operation stability. In general, the work of this paper shows that the device level real-time data fusion method for enhanced monitoring has clear technical value and engineering application prospect, which can provide reliable support for high-precision perception and rapid response of distributed energy grid.

## 6 Conclusion

Focusing on the requirements of enhanced monitoring of distributed energy grid, this paper constructs a real-time data fusion method at the device level, which completes the temporal alignment and unified representation of multi-source heterogeneous data, the state estimation and dynamic weighted fusion for real-time perception, and the closed-loop design of edge collaborative execution and monitoring output. At the method level, the joint modeling of lightweight convolution and GRU, quality-aware weight update, ring cache queue, priority scheduling and cloud-edge parameter synchronization mechanism are introduced to improve the computing continuity and edge deployability of the monitoring link. Experiments show that the proposed method is superior to single source monitoring and static weighted fusion in terms of monitoring accuracy, edge response efficiency and robustness under complex disturbances. The accuracy reaches 96.5%, the average response delay is 54 ms, and the number of processing Windows per unit time is increased to 18.6. It still maintains a relatively stable anomaly recognition ability under strong noise and packet loss conditions. The research results show that the proposed method can provide an effective technical path for distributed energy grid from data access to real-time understanding, rapid response and intelligent decision-making.

## References

- [1] Ganjkhani, M., Gilanifar, M., Giraldo, J., Parvania, M. Integrated Cyber and Physical Anomaly Location and Classification in Power Distribution Systems. *IEEE Transactions on Industrial Informatics*, 2021, 17(10): 7040–7049. DOI: 10.1109/TII.2021.3065080.

- [2] Khan, M. M. S., Giraldo, J., Parvania, M. Attack Detection in Power Distribution Systems Using a Cyber-Physical Real-Time Reference Model. *IEEE Transactions on Smart Grid*, 2022, 13(2): 1490–1499. DOI: 10.1109/TSG.2021.3128034.
- [3] Ahmed, A., Sadanandan Sajan, K., Srivastava, A. K., Wu, Y. Anomaly Detection, Localization and Classification Using Drifting Synchrophasor Data Streams. *IEEE Transactions on Smart Grid*, 2021, 12(4): 3570–3580. DOI: 10.1109/TSG.2021.3054375.
- [4] Ganjkhani, M., Gholami, A., Giraldo, J., Srivastava, A. K., Parvania, M. Multi-Source Data Aggregation and Real-Time Anomaly Classification and Localization in Power Distribution Systems. *IEEE Transactions on Smart Grid*, 2024, 15(2): 2191–2202. DOI: 10.1109/TSG.2023.3316548.
- [5] Gholami, A., Srivastava, A. K. ORCA: Outage Root Cause Analysis in DER-Rich Power Distribution System Using Data Fusion, Hierarchical Clustering and FP-Growth Rule Mining. *IEEE Transactions on Smart Grid*, 2024, 15(1): 667–676. DOI: 10.1109/TSG.2023.3281489.
- [6] Vosughi, A., Pannala, S., Srivastava, A. K. Event Detection, Classification and Localization in an Active Distribution Grid Using Data-Driven System Identification, Weighted Voting and Graph. *IEEE Transactions on Smart Grid*, 2023, 14(3): 1843–1854. DOI: 10.1109/TSG.2022.3213255.
- [7] Palomino, A., Giraldo, J., Parvania, M. Graph-Based Interdependent Cyber-Physical Risk Analysis of Power Distribution Networks. *IEEE Transactions on Power Delivery*, 2023, 38(3): 1510–1520. DOI: 10.1109/TPWRD.2022.3230926.
- [8] Jithish, J., Alangot, B., Mahalingam, N., Yeo, K. S. Distributed Anomaly Detection in Smart Grids: A Federated Learning-Based Approach. *IEEE Access*, 2023, 11: 7157–7179. DOI: 10.1109/ACCESS.2023.3237554.
- [9] Siniosoglou, I., Radoglou-Grammatikis, P., Efstathopoulos, G., Fouliras, P., Sarigiannidis, P. A Unified Deep Learning Anomaly Detection and Classification Approach for Smart Grid Environments. *IEEE Transactions on Network and Service Management*, 2021, 18(2): 1137–1151. DOI: 10.1109/TNSM.2021.3078381.
- [10] Oroza, C. A., Giraldo, J., Parvania, M., Watteyne, T. Wireless-Sensor Network Topology Optimization in Complex Terrain: A Bayesian Approach. *IEEE Internet of Things Journal*, 2021, 8(24): 17429–17435. DOI: 10.1109/JIOT.2021.3082168.
- [11] Irfan, M., Sadighian, A., Tanveer, A., Al-Naimi, S. J., Oligeri, G. A Survey on Detection and Localisation of False Data Injection Attacks in Smart Grids. *IET Cyber-Physical Systems: Theory & Applications*, 2024, 9(4): 313–333. DOI: 10.1049/cps2.12093.
- [12] Cárdenas, R., Arroba, P., Risco-Martín, J. L., Moya, J. M. Modeling and Simulation of Smart Grid-Aware Edge Computing Federations. *Cluster Computing*, 2023, 26(1): 719–743. DOI: 10.1007/s10586-022-03797-8.
- [13] Khaledian, E., Pandey, S., Kundu, P. Real-Time Synchrophasor Data Anomaly Detection and Classification Using Isolation Forest, KMeans, and LoOP. *IEEE*

- Transactions on Smart Grid, 2021, 12(3): 2378–2388. DOI: 10.1109/TSG.2020.3046602.
- [14] Gholami, A., Vosughi, A., Srivastava, A. K. Denoising and Detection of Bad Data in Distribution Phasor Measurements Using Filtering, Clustering, and Koopman Mode Analysis. *IEEE Transactions on Industry Applications*, 2022, 58(2): 1602–1610. DOI: 10.1109/TIA.2022.3145774.
- [15] Mehmood, M. Y., Oad, A., Abrar, M., Munir, H. M., Alhussein, M., Aurangzeb, K., Haider, S. I. Edge Computing for IoT-Enabled Smart Grid. *Security and Communication Networks*, 2021: 1–16, Article ID 5524025. DOI: 10.1155/2021/5524025.
- [16] Müller, N., Bao, K., Heussen, K. Cyber–physical Event Reasoning for Distributed Energy Resources. *Sustainable Energy, Grids and Networks*, 2024, 39: 101400. DOI: 10.1016/j.segan.2024.101400.
- [17] Vosughi, A., Tamimi, A., King, A. B., Majumder, S., Srivastava, A. K. Cyber–physical Vulnerability and Resiliency Analysis for DER Integration: A Review, Challenges and Research Needs. *Renewable and Sustainable Energy Reviews*, 2022, 168: 112794. DOI: 10.1016/j.rser.2022.112794.
- [18] Nikam, V., Kalkhambkar, V. A Review on Control Strategies for Microgrids with Distributed Energy Resources, Energy Storage Systems, and Electric Vehicles. *International Transactions on Electrical Energy Systems*, 2021, 31(1): e12607. DOI: 10.1002/2050-7038.12607.
- [19] Adham, M., Keene, S., Bass, R. B. Distributed Energy Resources: A Systematic Literature Review. *Energy Reports*, 2025, 13: 1980–1999. DOI: 10.1016/j.egyr.2025.01.026.
- [20] Hargroves, K., James, B., Lane, J., Newman, P. The Role of Distributed Energy Resources and Associated Business Models in the Decentralised Energy Transition: A Review. *Energies*, 2023, 16(10): 4231. DOI: 10.3390/en16104231.
- [21] Lakshmi Satya Nagasri, D., Marimuthu, R. Review on Advanced Control Techniques for Microgrids. *Energy Reports*, 2023, 10: 3054–3072. DOI: 10.1016/j.egyr.2023.09.162.
- [22] Islam, R., Rivin, M. A. H., Sultana, S., Asif, M. A. B., Mohammad, M., Rahaman, M. Machine Learning for Power System Stability and Control. *Results in Engineering*, 2025, 26: 105355. DOI: 10.1016/j.rineng.2025.105355.
- [23] Guato Burgos, M. F., Morato, J., Vizcaino Imacaña, F. P. A Review of Smart Grid Anomaly Detection Approaches Pertaining to Artificial Intelligence. *Applied Sciences*, 2024, 14(3): 1194. DOI: 10.3390/app14031194.
- [24] Ojo, K. E., Saha, A. K., Srivastava, V. M. Microgrids’ Control Strategies and Real-Time Monitoring Systems: A Comprehensive Review. *Energies*, 2025, 18(13): 3576. DOI: 10.3390/en18133576.

- [25] Alvarez-Alvarado, M. S., Apolo-Tinoco, C., Ramirez-Prado, M. J., Alban-Chacón, F. E., Pico, N., Aviles-Cedeno, J., Recalde, A. A., Moncayo-Rea, F., Velasquez, W., Rengifo, J. Cyber-physical Power Systems: A Comprehensive Review about Technologies Drivers, Standards, and Future Perspectives. *Computers & Electrical Engineering*, 2024, 116: 109149. DOI: 10.1016/j.compeleceng.2024.109149.
- [26] Alrowaili, Y., Saxena, N., Srivastava, A., Conti, M., Burnap, P. A Review: Monitoring Situational Awareness of Smart Grid Cyber-Physical Systems and Critical Asset Identification. *IET Cyber-Physical Systems: Theory & Applications*, 2023, 8(3): 160–185. DOI: 10.1049/cps2.12059.
- [27] Menazzi, M., Qin, C., Srivastava, A. K. Enabling Resiliency Through Outage Management and Data-Driven Real-Time Aggregated DERs. *IEEE Transactions on Industry Applications*, 2023, 59(5): 5728–5738. DOI: 10.1109/TIA.2023.3285516.